IEEE Access
Multidisciplinary ⋮ Rapid Review ⋮ Open Access Journal

Received March 17, 2019, accepted April 7, 2019, date of publication April 12, 2019, date of current version April 29, 2019.

Digital Object Identifier 10.1109/ACCESS.2019.2910889

Joint 2-D DOA and Doppler Estimation for L-Shaped Array via Dual PARAFAC With Triple Matching Implementation

RIHENG WU[1], (Member, IEEE), LE XU[2], ZHENHAI ZHANG[3], AND YANGYANG DONG[4]

[1]Department of Information Engineering, Wenjing College, Yantai University, Yantai 264005, China
[2]College of Electronic and Information Engineering, Nanjing University of Aeronautics and Astronautics, Nanjing 210000, China
[3]School of Mechatronics Engineering, Beijing Institute of Technology, Beijing 100081, China
[4]School of Electrical Engineering, Xidian University, Xi'an 710071, China

Corresponding author: Riheng Wu (riheng_w@163.com)

This work was supported in part by the Shandong Province NSF under Grant ZR2016FM43, in part by the China NSF under Grant 61371169 and Grant 61773059, in part by the National Defense Major Fundamental Research Program of China under Grant C× × ×20110003, in part by the National Defense Key Fundamental Research Program of China under Grant A× × ×20110005 and Grant A × × ×20132010, in part by the Natural Science Basic Research Project of Shaanxi Province under Grant 2018JQ6046, and in part by the China Postdoctoral Science Foundation under Grant 2017M623123.

ABSTRACT A dual parallel factor (PARAFAC)-based approach to jointly estimating the two-dimensional direction of arrival (2-D DOA) and Doppler is proposed in this paper, where an L-shaped array consisting of acoustic vector-sensor is used. First, we apply the PARAFAC decomposition to the data model formed by concatenating the outputs of multi-level delays of the observations, and we get the parameter matrix H, which accomplish the 2-D DOA estimation and pairing automatically, then the dual PARAFAC decomposition is applied to the achieved composite steering matrix from the first PARAFAC decomposition, and thus, the same permutation matrices link the estimates of steering matrices and delay matrices from X-subarray and Y-subarray, respectively. Following this, the Doppler and 2-D DOA matching information are obtained via triple matching implementation, e.g. 2-D DOA and frequency matching. Finally, Doppler is estimated by delay matrices. The proposed algorithm is computationally effective for both uniform and non-uniform L-shaped array as SNR exceeds 15dB, and its performance outperforms the joint angle and Doppler shift ESPRIT (JAD-ESPRIT) algorithm and the joint angle and Doppler shift PM (JAD-PM) algorithm. The simulation results justified the effectiveness of the proposed algorithm.

INDEX TERMS Two-dimensional direction of arrival (2-D DOA), Doppler, L-shaped array, dual parallel factor (PARAFAC), triple matching implementation.

I. INTRODUCTION

In recent decades, array signal processing has made rapid progress in many fields, e.g., radar, sonar, satellite communication and so on [1]–[3]. Joint multi-parameter estimation has been one of the fundamental problems in array signal processing society and has aroused considerable concerns [4], [5]. For such a problem, the observations from the array output often contain multiple parameters to be estimated and matched synchronously. Many multi-parameter estimation methods have been proposed recently [4]–[11], exiting popular high-resolution methods used to jointly estimate the angles and carrier frequency include multiple signal classification (MUSIC) algorithm [6], estimating signal parameters via rotational invariance techniques (ESPRIT) algorithm [1], [19], [20], Propagator method (PM) [8] and parallel factor (PARAFAC) method [9], [10]. However, all these methods have limitations to estimate Doppler when sources are moving, for instance, in ELINT, the radar could be installed on a moving platform, which yields the Doppler when the radar is moving towards or moving away from the receiver, such scenarios pose the joint 2-D DOA and Doppler estimation a challenging question. Ying and Leus proposed a space-time compressive sampling (STCS) array architecture to estimate

The associate editor coordinating the review of this manuscript and approving it for publication was Liangtian Wan.

Doppler-DOA by exploiting the sparsity in the angle and frequency domain [12]. Min *et al*. developed structure of transmitted signals and applied PRO-ESPRIT to joint time delays, DOAs and Doppler shifts estimations [13]. However, joint 2-D DOA and Doppler estimation is still a challenging problem.

In order to address joint 2-D DOA and Doppler estimation, we propose a dual PARAFAC method to achieve paired 2-D DOA and Doppler via triple matching implementation, where the L-shaped array consisting of acoustic vector sensors is used. Compared to conventional sensor arrays, acoustic vector sensors can measure the acoustic pressure as well as all three orthogonal components of the acoustic particle velocity [14], [15]. To estimate Doppler, the proposed method introduces multi-level delays of the observations from L-shaped array. The procedure to estimate Doppler from parameters matrices can be implemented via dual PARAFAC decomposition. Eventually, the 2-D DOA and Doppler together with the carrier frequency can be estimated and paired by triple matching implementation. The main contributions of our research are summarized as follows:

1) We generalize the PARAFAC analysis and propose a dual PARAFAC model, which is suitable to descript multi-level delay outputs of L-shaped array configured with acoustic vector-sensors.

2) We obtain the 2-D DOA and Doppler estimation from the dual PARAFAC model via dual PARAFAC decomposition.

3) We propose a triple matching implementation to obtain the paired 2-D DOA, Doppler and carrier frequency.

4) The parameters estimation performance of the proposed algorithm outperforms the joint angle and Doppler shift ESPRIT (JAD-ESPRIT) algorithm and joint angle and Doppler shift PM (JAD-PM) algorithm which can be extended from [7] and [8].

The remainder of our paper is organized as follows: Section II presents the dual PARAFAC model of multi-level delay outputs for L-shaped array. Based on this model, Section III derives the proposed algorithm as well as the parameters matching approach. Section IV gives the complexity analysis of the proposed algorithm. Numerical simulations are showed in Section V to demonstrate the performance of the proposed approach and we conclude this paper in section VI.

Notation: Matrices and vectors are represented by boldfaced capital letters and lower case letters respectively. $\otimes$, $\odot$ and $\oplus$ denote *Kronecker* product, *Khatri–Rao* product and *Hadamard* product, respectively. $(\cdot)^*$, $(\cdot)^T$, $(\cdot)^H$ and $(\cdot)^{-1}$ denote complex conjugation, transpose, conjugate-transpose and inverse, respectively. $(\cdot)^\dagger$ denotes the Moore-Penrose pseudoinverse. $\|\cdot\|_F$ and $\|\cdot\|_0$ represent the *Forbenius* norm and l_0–norm. $D_n(\mathbf{A})$ denotes a diagonal matrix consisting of the$n$-th row of $\mathbf{A}$. $abs(\cdot)$ the modulus value symbol and $angle(\cdot)$ the phase angle operator.

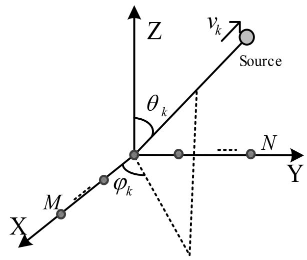

FIGURE 1. The structure of the L-shaped array.

II. DATA MODEL

Assume that there are K moving signals impinge on an L-shaped array consisting of two orthogonal M-element and N-element linear acoustic vector-sensor arrays along x-axis and y-axis, respectively. The reference element is placed at the origin and the sources are moving in line with the origin. The distance between m-th sensor and the reference element ($m = 1$) is d_m^x, while the distance between n-th sensor and the reference element ($n = 1$) is d_n^y. The structure of the L-shaped array is shown in Fig. 1.

Assume that the received noise is additive white Gaussian and independent to the incident signals. The K signals are all uncorrelated narrow-band plane waves propagating from far-field with known but different center frequency $(f_1, f_2, \ldots, f_K)$. The velocity and the angle paring of the k-th signal is v_k and (φ_k, θ_k), respectively, where φ_k and θ_k are the azimuth angle and elevation angle. The outputs of X-subarray and Y-subarray at the t-th snapshot can be respectively modeled as [16]

$$\mathbf{x}_0(t) = [\mathbf{A}_x \odot \mathbf{H}]\mathbf{s}(t) + \mathbf{n}_x(t), \tag{1}$$

$$\mathbf{y}_0(t) = [\mathbf{A}_y \odot \mathbf{H}]\mathbf{s}(t) + \mathbf{n}_y(t), \tag{2}$$

where $\mathbf{s}(t) = [s_1(t), s_2(t), \cdots, s_K(t)]^T$ is the envelope vector of K signals. $\mathbf{A}_x^{M\times K} = [\mathbf{a}_x(\varphi_1, \theta_1, f_1), \cdots, \mathbf{a}_x(\varphi_K, \theta_K, f_K)]$ is the steering matrix of X-subarray, where $\mathbf{a}_x(\varphi_k, \theta_k, f_k) = [1, \exp(-j2\pi d_2^x f_k \cos\varphi_k \sin\theta_k/c), \cdots, \exp(-j2\pi d_M^x f_k \cos\varphi_k \sin\theta_k/c)]^T$. $\mathbf{A}_y^{N\times K} = [\mathbf{a}_y(\varphi_1, \theta_1, f_1), \cdots, \mathbf{a}_y(\varphi_K, \theta_K, f_K)]$ is the steering matrix of Y-subarray, where $\mathbf{a}_y(\varphi_k, \theta_k, f_k) = [1, \exp(-j2\pi d_2^y f_k \sin\varphi_k \sin\theta_k/c), \cdots, \exp(-j2\pi d_N^y f_k \sin\varphi_k \sin\theta_k/c)]^T$. $\mathbf{H} = [\mathbf{h}_1, \mathbf{h}_2, \cdots, \mathbf{h}_K] \in \mathbb{C}^{4\times K}$ is the $4 \times K$ location vector of K signals, and $\mathbf{h}_k = [1, \cos\varphi_k \sin\theta_k, \sin\varphi_k \sin\theta_k, \cos\theta_k]^T$. c denotes the signal propagation velocity, $\mathbf{n}_x(t) \in \mathbb{C}^{M\times 1}$, $\mathbf{n}_y(t) \in \mathbb{C}^{N\times 1}$ denote the $M \times 1$ and $N \times 1$ noise vector from X-subarray and Y-subarray, respectively.

To estimate the frequency, we introduce the structure of multi-level delays following the output of the array. As is shown in Fig. 2, we consider $P - 1$ levels delay where the p-th delay is $\tau_p = p\tau$ and τ satisfies $0 < \tau < 1/(P - 1)\max(f_k)$[17].

Given the p-th delay τ_p, the output of the p-th delay of X-subarray can be written as [8]

$$\mathbf{x}_p(t) = \mathbf{x}_0(t - p\tau)$$

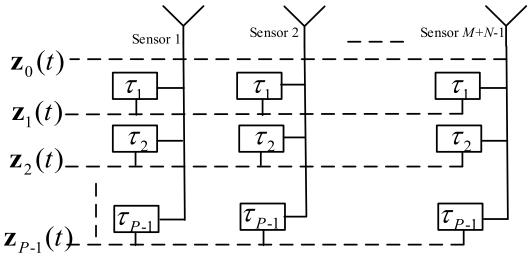

FIGURE 2. The structure of multi-level delay after the sensors array.

$$\begin{aligned} &= [\mathbf{A}_x \odot \mathbf{H}]\mathbf{s}(t-p\tau) + \mathbf{n}_x(t-p\tau) \\ &= [\mathbf{A}_x \odot \mathbf{H}]D_{p+1}(\mathbf{F}_x)\mathbf{s}(t) + \mathbf{n}_{xp}(t). \end{aligned} \tag{3}$$

where $\mathbf{n}_{xp}(t) = \mathbf{n}_x(t-p\tau)$ is the p-th delay noise, $\mathbf{F}_x$ is the delay matrix defined in Appendix A.

Given J snapshots $[\mathbf{x}_p(t_1), \mathbf{x}_p(t_2), \ldots, \mathbf{x}_p(t_J)]$, and let $\mathbf{X}_p = [\mathbf{x}_p(t_1), \mathbf{x}_p(t_2), \ldots, \mathbf{x}_p(t_J)]$, then $\mathbf{X}_p$ can be written as

$$\mathbf{X}_p = [\mathbf{A}_x \odot \mathbf{H}]D_{p+1}(\mathbf{F}_x)\mathbf{S}^T + \mathbf{N}_{xp}, \tag{4}$$

where $\mathbf{S}^{J\times K}\mathbf{s}(t_1), \mathbf{s}(t_2), \ldots, \mathbf{s}(t_J)^T$, $\mathbf{N}_{xp}\mathbf{n}_{xp}(t_1), \mathbf{n}_{xp}(t_2), \ldots, \mathbf{n}_{xp}(t_J)$. By concatenating the outputs from P levels delay of X-subarray in a column way, we obtain a new data matrix

$$\begin{aligned} \mathbf{X}^{4MP\times J} &= \begin{bmatrix} \mathbf{X}_0 \\ \mathbf{X}_1 \\ \vdots \\ \mathbf{X}_{P-1} \end{bmatrix} = \begin{bmatrix} [\mathbf{A}_x \odot \mathbf{H}]D_1(\mathbf{F}_x) \\ [\mathbf{A}_x \odot \mathbf{H}]D_2(\mathbf{F}_x) \\ \vdots \\ [\mathbf{A}_x \odot \mathbf{H}]D_P(\mathbf{F}_x) \end{bmatrix} \mathbf{S}^T + \begin{bmatrix} \mathbf{N}_{x0} \\ \mathbf{N}_{x1} \\ \vdots \\ \mathbf{N}_{xP-1} \end{bmatrix} \\ &= [\mathbf{F}_x \odot \mathbf{A}_x \odot \mathbf{H}]\mathbf{S}^T + \mathbf{N}_x, \end{aligned} \tag{5}$$

where $\mathbf{N}_x = [\mathbf{N}_{x0}^T, \mathbf{N}_{x1}^T, \ldots, \mathbf{N}_{xP-1}^T]^T$ is the noise matrix of X-subarray. Similarly, the outputs from P levels delays of Y-subarray is written as

$$\mathbf{Y}^{4NP\times J} = [\mathbf{F}_y \odot \mathbf{A}_y \odot \mathbf{H}]\mathbf{S}^T + \mathbf{N}_y, \tag{6}$$

where $\mathbf{N}_y = [\mathbf{N}_{y0}^T, \mathbf{N}_{y1}^T, \ldots, \mathbf{N}_{yP-1}^T]^T$ is the noise matrix of Y-subarray, and $\mathbf{F}_y$ is the delay matrix defined in Appendix B.

By stacking $\mathbf{X}$ and $\mathbf{Y}$ in a data matrix, we have the final received data matrix

$$\begin{aligned} \mathbf{Z} &= \begin{bmatrix} \mathbf{X} \\ \mathbf{Y} \end{bmatrix} = \begin{bmatrix} \mathbf{F}_x \odot \mathbf{A}_x \odot \mathbf{H} \\ \mathbf{F}_y \odot \mathbf{A}_y \odot \mathbf{H} \end{bmatrix} \mathbf{S}^T + \begin{bmatrix} \mathbf{N}_x \\ \mathbf{N}_y \end{bmatrix} \\ &= \left[\begin{pmatrix} \mathbf{F}_x \odot \mathbf{A}_x \\ \mathbf{F}_y \odot \mathbf{A}_y \end{pmatrix} \odot \mathbf{H} \right] \mathbf{S}^T + \mathbf{N}. \end{aligned} \tag{7}$$

III. JOINT 2-D DOA AND DOPPLER ESTIMATION

In this Section, we first propose the dual PARAFAC decomposition, the aim of which is twofold: the first one is to achieve automatic paired 2-D DOA estimation, and the second is to establish the mappings between estimates and ground truth of both steering matrices and delay matrices. We then estimate Doppler and investigate the pairing procedure of 2-D DOA, carrier frequency and Doppler via triple matching implementation.

Trilinear alternating least square (TALS) algorithm is an efficient method for the decomposition of PARAFAC model [11]. The basic idea of TALS is to update one matrix in PARAFAC model each time until convergence. Based on TALS, we propose a novel dual PARAFAC decomposition algorithm to obtain the estimates of parameters matrices in $\mathbf{Z}$, and achieve the paired 2-D DOA, frequency and Doppler via triple matching implementation.

A. DUAL PARAFAC DECOMPOSITION

1) THE FIRST PARAFAC DECOMPOSITION AND ANGLES ESTIMATION

Let $\mathbf{B} = \begin{bmatrix} \mathbf{F}_x \odot \mathbf{A}_x \\ \mathbf{F}_y \odot \mathbf{A}_y \end{bmatrix}$, Eq. (7) can be rewritten as

$$\mathbf{Z}_I = [\mathbf{B} \odot \mathbf{H}]\,\mathbf{S}^T + \mathbf{N}. \tag{8}$$

In the noise free case, the can be written as the PARAFAC model [9]

$$\begin{aligned} z_{pm+pn,j,q} &= \sum_{k=1}^{K} \mathbf{B}(pm+pn, k)\mathbf{S}(j,k)\mathbf{H}(q,k) \\ m &= 1, \ldots, M; \quad n = 1, \ldots, N;\ j = 1, \ldots, J; \\ p &= 1, \ldots, P; \quad q = 1, 2, 3, 4, \end{aligned} \tag{9}$$

where $\mathbf{B}(pm+pn, k)$ is the $(pm+pn, k)^{th}$ element of $\mathbf{B}$, $\mathbf{S}(j, k)$ is the $(j, k)^{th}$ element of $\mathbf{S}$ and $\mathbf{H}(q, k)$ is the $(q, k)^{th}$ element of $\mathbf{H}$. The structure of the PARAFAC model in (9) implies two other rearranged matrices

$$\mathbf{Z}_{II} = [\mathbf{S} \odot \mathbf{B}]\mathbf{H}^T + \mathbf{N}_{II}, \tag{10}$$

$$\mathbf{Z}_{III} = [\mathbf{H} \odot \mathbf{S}]\mathbf{B}^T + \mathbf{N}_{III}, \tag{11}$$

Apply the LS fitting to (8), we have

$$\min_{\mathbf{B},\mathbf{H},\mathbf{S}} \left\| \mathbf{Z}_I - [\mathbf{B} \odot \mathbf{H}]\mathbf{S}^T \right\|_F, \tag{12}$$

The LS update for $\mathbf{S}$ is

$$\hat{\mathbf{S}}^T = [\hat{\mathbf{B}} \odot \hat{\mathbf{H}}]^\dagger \mathbf{Z}_I, \tag{13}$$

where $\hat{\mathbf{B}}$ and $\hat{\mathbf{H}}$ are the previous estimates of $\mathbf{B}$ and $\mathbf{H}$, respectively.

Apply the LS fitting to (10), we have

$$\min_{\mathbf{B},\mathbf{H},\mathbf{S}} \left\| \mathbf{Z}_{II} - [\mathbf{S} \odot \mathbf{B}]\mathbf{H}^T \right\|_F, \tag{14}$$

The LS update for $\mathbf{H}$ is

$$\hat{\mathbf{H}}^T = [\hat{\mathbf{S}} \odot \hat{\mathbf{B}}]^\dagger \mathbf{Z}_{II}, \tag{15}$$

where $\hat{\mathbf{B}}$ and $\hat{\mathbf{S}}$ are the previous estimates of $\mathbf{B}$ and $\mathbf{S}$, respectively.

Apply the LS fitting to (11), we have

$$\min_{\mathbf{B},\mathbf{H},\mathbf{S}} \left\| \mathbf{Z}_{III} - [\mathbf{H} \odot \mathbf{S}]\mathbf{B}^T \right\|_F, \tag{16}$$

The LS update for $\mathbf{B}$ is

$$\hat{\mathbf{B}}^T = [\hat{\mathbf{H}} \odot \hat{\mathbf{S}}]^\dagger \mathbf{Z}_{III}, \tag{17}$$

where $\hat{\mathbf{H}}$ and $\hat{\mathbf{S}}$ are the previous estimates of $\mathbf{H}$ and $\mathbf{S}$, respectively.

Note: the noise term $\mathbf{N}$ in Eq. (7) after multi-level delays might be correlated, which causes samples covariance matrix to be non-diagonal uniform matrix, which could degrade the performance of all comparable methods and CRB as well. To obtain parameters MVU estimation, a pre-whitening transformation or decorrelation processing is necessary. For instance, $\mathbf{N} \sim \mathbb{N}(\mathbf{0}, \mathbf{C})$, let $\mathbf{C}^{-1} = \mathbf{D}^T\mathbf{D}$, $\mathbf{D}$ is the invertible matrix, we have $E[(\mathbf{DN})(\mathbf{DN})^T] = \mathbf{DCD}^T = \mathbf{DD}^{-1}\mathbf{D}^{T^{-1}}\mathbf{D}^T = \mathbf{I}$, let $\mathbf{Z}' = \mathbf{DZ}$, we complete the decorrelation processing.

For the PARAFAC decomposition, we first utilize Gaussian random matrix to initialize the parameter matrices $\mathbf{B}$, $\mathbf{H}$, $\mathbf{S}$ and repeatedly update them until convergence. Define the sum of squared residuals (SSR) of the k-th decomposition by

$$SSR_k = \sum_{i=1}^{4(PM+PN)} \sum_{j=1}^{J} \left|c_{ij}\right|^2, \tag{18}$$

where c_{ij} is the $(i,j)^{th}$ element of $\mathbf{C} = \mathbf{Z} - [\hat{\mathbf{B}} \odot \hat{\mathbf{H}}]\hat{\mathbf{S}}^T$. Define the convergence speed of the PARAFAC decomposition as $SSR_{rate} = (SSR_k - SSR_{k-1})\big/SSR_{k-1}$. When SSR_{rate} is smaller than a certain small value, the iteration process is terminated.

The uniqueness of the PARAFAC decomposition can be guaranteed since the k-rank [18] condition $k_{\mathbf{B}} + k_{\mathbf{S}} + k_{\mathbf{H}} \geq 2K + 2$ is satisfied [7] where $k_{\mathbf{B}}$, $k_{\mathbf{S}}$ and $k_{\mathbf{H}}$ are the k-rank of $\mathbf{B}$, $\mathbf{S}$ and $\mathbf{H}$, respectively. The estimates of $\mathbf{B}$, $\mathbf{H}$ and $\mathbf{S}$ can be expressed as

$$\hat{\mathbf{B}} = \mathbf{B}\Pi_1\mathbf{\Delta}_1 + \mathbf{W}_1, \tag{19}$$
$$\hat{\mathbf{H}} = \mathbf{H}\Pi_1\mathbf{\Delta}_2 + \mathbf{W}_2, \tag{20}$$
$$\hat{\mathbf{S}} = \mathbf{S}\Pi_1\mathbf{\Delta}_3 + \mathbf{W}_3, \tag{21}$$

where $\mathbf{\Pi}_1$denotes the permutation matrix, $\mathbf{\Delta}_1$, $\mathbf{\Delta}_2$ and $\mathbf{\Delta}_3$ are the diagonal scaling matrix satisfying $\mathbf{\Delta}_1\mathbf{\Delta}_2\mathbf{\Delta}_3 = \mathbf{I}$. $\mathbf{W}_1$, $\mathbf{W}_2$ and $\mathbf{W}_3$ are the estimation errors. Scale ambiguity in $\hat{\mathbf{B}}$ and $\hat{\mathbf{H}}$ can be eliminated by dividing each column of the matrices by its first element, respectively.

Define $r_k = \hat{\mathbf{h}}_k(2) + j\hat{\mathbf{h}}_k(3)$, j is the image number unit, $\hat{\mathbf{h}}_k(2)$ and $\hat{\mathbf{h}}_k(3)$ are the second and third row of $\hat{\mathbf{h}}_k$, respectively, the estimates of 2-D DOA are achieved by

$$\hat{\varphi}_{c_k} = angle(r_k) \quad k = 1, 2, \cdots, K, \tag{22}$$
$$\hat{\theta}_{c_k} = \sin^{-1}(abs(r_k)), \quad k = 1, 2, \cdots, K. \tag{23}$$

Since we have estimated both azimuth and elevation angles from the same column of $\hat{\mathbf{H}}$, the angles paring procedure is completed automatically.

2) THE SECOND PARAFAC DECOMPOSITION

Under the noiseless case, $\hat{\mathbf{B}}$ is further written as

$$\hat{\mathbf{B}} = \begin{bmatrix} \hat{\mathbf{F}}_x \odot \hat{\mathbf{A}}_x \\ \hat{\mathbf{F}}_y \odot \hat{\mathbf{A}}_y \end{bmatrix} \mathbf{\Pi}_1 = \begin{bmatrix} \hat{\mathbf{F}}_x\mathbf{\Pi}_1 \odot \hat{\mathbf{A}}_x\mathbf{\Pi}_1 \\ \hat{\mathbf{F}}_y\mathbf{\Pi}_1 \odot \hat{\mathbf{A}}_y\mathbf{\Pi}_1 \end{bmatrix} = \begin{bmatrix} \hat{\mathbf{B}}_x \\ \hat{\mathbf{B}}_y \end{bmatrix}, \tag{24}$$

where $\hat{\mathbf{B}}_x = \hat{\mathbf{F}}_x\mathbf{\Pi}_1 \odot \hat{\mathbf{A}}_x\mathbf{\Pi}_1$ isthe first $P \times M$ rows of $\hat{\mathbf{B}}$ and $\hat{\mathbf{B}}_y = \hat{\mathbf{F}}_y\mathbf{\Pi}_1 \odot \hat{\mathbf{A}}_y\mathbf{\Pi}_1$ is the last $P \times N$ rows of $\hat{\mathbf{B}}$. Define two matrices $\mathbf{G}_x$ and $\mathbf{G}_y$ as

$$\begin{aligned} \mathbf{G}_x &= \left(\hat{\mathbf{B}}_x^T\right)^{\dagger} = \left(((\mathbf{F}_x \odot \mathbf{A}_x)\,\mathbf{\Pi}_1)^T\right)^{\dagger} \\ &= ((\mathbf{F}_x\mathbf{\Pi}_1) \odot (\mathbf{A}_x\mathbf{\Pi}_1)) \left[\mathbf{\Pi}_1(\mathbf{F}_x^T\mathbf{F}_x) \oplus (\mathbf{A}_x^T\mathbf{A}_x)\mathbf{\Pi}_1\right] \\ &= (\mathbf{F}_x\mathbf{\Pi}_1 \odot \mathbf{A}_x\mathbf{\Pi}_1)\mathbf{D}_x^T, \end{aligned} \tag{25}$$

$$\begin{aligned} \mathbf{G}_y &= \left(\hat{\mathbf{B}}_y^T\right)^{\dagger} = \left(\left((\mathbf{F}_y \odot \mathbf{A}_y)\,\mathbf{\Pi}_1\right)^T\right)^{\dagger} \\ &= \left((\mathbf{F}_y\mathbf{\Pi}_1) \odot (\mathbf{A}_y\mathbf{\Pi}_1)\right) \left[\mathbf{\Pi}_1(\mathbf{F}_y^T\mathbf{F}_y) \oplus (\mathbf{A}_y^T\mathbf{A}_y)\mathbf{\Pi}_1\right] \\ &= (\mathbf{F}_y\mathbf{\Pi}_1 \odot \mathbf{A}_y\mathbf{\Pi}_1)\mathbf{D}_y^T, \end{aligned} \tag{26}$$

where $\mathbf{D}_x[\mathbf{\Pi}_1(\mathbf{F}_x^T\mathbf{F}_x) \oplus (\mathbf{A}_x^T\mathbf{A}_x)\mathbf{\Pi}_1]^T$, $\mathbf{D}_y = [\mathbf{\Pi}_1(\mathbf{F}_y^T\mathbf{F}_y) \oplus (\mathbf{A}_y^T\mathbf{A}_y)\mathbf{\Pi}_1]^T$. Apply PARAFAC decomposition to Eq. (25) and Eq. (26), after elimination of scale ambiguity, we can obtain estimates of $\mathbf{A}_x$, $\mathbf{F}_x$, $\mathbf{A}_y$ and $\mathbf{F}_y$

$$\hat{\mathbf{A}}_x = \mathbf{A}_x\mathbf{\Pi}_2 + \mathbf{W}_{11}, \quad \hat{\mathbf{F}}_x = \mathbf{F}_x\mathbf{\Pi}_2 + \mathbf{W}_{12}, \tag{27}$$
$$\hat{\mathbf{A}}_y = \mathbf{A}_y\mathbf{\Pi}_3 + \mathbf{W}_{13}, \quad \hat{\mathbf{F}}_y = \mathbf{F}_y\mathbf{\Pi}_3 + \mathbf{W}_{14}, \tag{28}$$

where $\mathbf{\Pi}_2$ and $\mathbf{\Pi}_3$ the permutation matrices, and $\mathbf{W}_{11}$, $\mathbf{W}_{12}$, $\mathbf{W}_{13}$ and $\mathbf{W}_{14}$ are the estimation noise. The uniqueness of the second PARAFAC decomposition can be guaranteed since the k-rank condition $k_{\mathbf{A}_x} + k_{\mathbf{F}_x} + k_{\mathbf{D}_x} \geq 2K + 2$ and $k_{\mathbf{A}_y} + k_{\mathbf{F}_y} + k_{\mathbf{D}_y} \geq 2K + 2$ are satisfied, respectively. *Note:* the uniqueness condition of PARAFAC decomposition can be guaranteed as long as the parameters matrices which can be written as the PARAFAC decomposition model are column full-rank.

B. TRIPLE MATCHING IMPLEMENTATION AND DOPPLER ESTIMATION

The columns of $\hat{\mathbf{H}}$ have $P_K = K!$ permutations, define $\boldsymbol{\rho}_{px} = \hat{\mathbf{H}}_p(2,:)$ and $\boldsymbol{\rho}_{py} = \hat{\mathbf{H}}_p(3,:)$ as the second and the third row of the p-th permutation of $\hat{\mathbf{H}}_p$, respectively. The elevation angles of p-th permutation are $\hat{\boldsymbol{\theta}}_p = [\hat{\theta}_{p1}, \cdots, \hat{\theta}_{pK}]$.

Define $\boldsymbol{\eta}_x^j = \kappa_x \left.\frac{\partial \boldsymbol{\rho}_{jx}}{\partial \cos\boldsymbol{\theta}_j}\right|_{\boldsymbol{\theta}_j=\hat{\boldsymbol{\theta}}_j, \varphi_j=\hat{\varphi}_j}$, $\boldsymbol{\eta}_y^j = \kappa_y \left.\frac{\partial \boldsymbol{\rho}_{jy}}{\partial \cos\boldsymbol{\theta}_j}\right|_{\boldsymbol{\theta}_j=\hat{\boldsymbol{\theta}}_j, \boldsymbol{\varphi}_j=\hat{\varphi}_j}$, where $\kappa_x = j2\pi d_2^x/c$, $\kappa_y = j2\pi d_2^y/c$, $\left.\frac{\partial \boldsymbol{\rho}_{jx}}{\partial \cos\boldsymbol{\theta}_j}\right|_{\boldsymbol{\theta}_j=\hat{\boldsymbol{\theta}}_j, \boldsymbol{\phi}_j=\hat{\phi}_j}$ and $\left.\frac{\partial \boldsymbol{\rho}_{jy}}{\partial \cos\boldsymbol{\theta}_j}\right|_{\boldsymbol{\theta}_j=\hat{\boldsymbol{\theta}}_j, \boldsymbol{\phi}_j=\hat{\phi}_j}$ are defined in Appendix C, respectively. Let $\mathbf{f}_i = [f_{i,1}, f_{i,2}, \cdots, f_{i,K}]$, $i = 1, \cdots, P_K$ be the i-th frequency permutation. To obtain the permutation matrices $\mathbf{\Pi}_2$ and $\mathbf{\Pi}_3$, we define

$$\boldsymbol{\mu}_x^{(i,j)} = e^{\mathbf{f}_i \oplus \boldsymbol{\eta}_x^j}, \quad i = 1, \cdots, P_K,\ j = 1, \cdots, P_K, \tag{29}$$
$$\boldsymbol{\mu}_y^{(i,j)} = e^{\mathbf{f}_i \oplus \boldsymbol{\eta}_y^j}, \quad i = 1, \cdots, P_K,\ j = 1, \cdots, P_K, \tag{30}$$

where $\boldsymbol{\mu}_x^{(i,j)}$ and $\boldsymbol{\mu}_y^{(i,j)}$ are determined by the angle and frequency combination $\{\boldsymbol{\theta}_j, \mathbf{f}_i\}_{i=1,j=1}^{P_K}$. Define $\hat{\mathbf{a}}_x^{(2)} = \hat{\mathbf{A}}_x(2,:)$ and $\hat{\mathbf{a}}_y^{(2)} = \hat{\mathbf{A}}_y(2,:)$ as the second row of $\hat{\mathbf{A}}_x$ and $\hat{\mathbf{A}}_y$, respectively. The projection of $\boldsymbol{\mu}_x^{(i,j)}$ and $\boldsymbol{\mu}_y^{(i,j)}$ on $\hat{\mathbf{a}}_x^{(2)*}$ and $\hat{\mathbf{a}}_y^{(2)*}$ can be expressed respectively as

$$I_x^{(i,j)} = <\boldsymbol{\mu}_x^{(i,j)}, \quad \hat{\mathbf{a}}_x^{(2)*}>= \boldsymbol{\mu}_x^{(i,j)} \cdot \hat{\mathbf{a}}_x^{(2)*}, \ i = 1, \cdots, P_K,$$

TABLE 1. Complexity of relevant algorithms.

Algorithm	Complexity
The proposed	$O[n_1(3K^2+K^2(J+PM+PN+4)+6K^2P((M+N)(4+J)+4J)+12KP(M+N)J)+n_{21}(3K^2+K^2(K+P+M)+6K^2(P(M+K)+MK)+3K^2PM)+n_{22}(3K^2+K^2(K+P+N)+6K^2(P(N+K)+NK)+3K^2PN)+2K(K!)+K^2(M+N)]$
JAD-PM	$O[JK^2+(4(M+N)P-K)K+(4(M+N)P-K)K^2+8((M+N)P-1)K^2+4(M+N)PK^2+2P(M+N-2)K^2+8K^3]$
JAD-ESPRIT	$O[16(M+N)^2P^2J+64(M+N)^3P^3+8((M+N)P-1)K^2+3K^3+4(M+N)PK^2+2P(M+N-2)K^2+4K^3]$

$$j=1,\cdots,P_K, \tag{31}$$

$$I_y^{(i,j)}=<\boldsymbol{\mu}_y^{(i,j)},\quad \hat{\mathbf{a}}_y^{(2)*}>=\boldsymbol{\mu}_y^{(i,j)}\cdot\hat{\mathbf{a}}_y^{(2)*},\ i=1,\cdots,P_K,\quad j=1,\cdots,P_K. \tag{32}$$

The optimal parings $\{\boldsymbol{\theta}_x^{opt},\mathbf{f}_x^{opt}\}$ or $\{\boldsymbol{\theta}_y^{opt},\mathbf{f}_y^{opt}\}$ should be those satisfying to maximize $I_x^{(i,j)}$ or $I_y^{(i,j)}$, namely,

$$\{\boldsymbol{\theta}_x^{opt},\mathbf{f}_x^{opt}\}=\arg\max_{\{\boldsymbol{\theta}_j,\mathbf{f}_i\}} I_x^{(i,j)},\ i=1,\cdots,P_K,\ j=1,\cdots,P_K, \tag{33}$$

$$\{\boldsymbol{\theta}_y^{opt},\mathbf{f}_y^{opt}\}=\arg\max_{\{\boldsymbol{\theta}_j,\mathbf{f}_i\}} I_y^{(i,j)},\ i=1,\cdots,P_K,\ j=1,\cdots,P_K. \tag{34}$$

Thus, we get the paired 2-D DOA and frequency, as well as the permutation information of $\hat{\mathbf{A}}_x$ and $\hat{\mathbf{A}}_y$. Since $\hat{\mathbf{F}}_x$ and $\hat{\mathbf{F}}_y$ share the same permutation matrix with $\hat{\mathbf{A}}_x$ and $\hat{\mathbf{A}}_y$, respectively, no additional paring procedure is needed for Doppler estimation.

Let the paired angles and frequency of $\hat{\mathbf{A}}_x$ be $[-\cos\hat{\varphi}_1^{opt,x}\sin\hat{\theta}_1^{opt,x},-\cos\hat{\varphi}_2^{opt,x}\sin\hat{\theta}_2^{opt,x},\cdots,-\cos\hat{\varphi}_K^{opt,x}]$ and $[f_1^{opt,x},\ldots,f_K^{opt,x}]$, let the paired angles and frequency of $\hat{\mathbf{A}}_y$ be $[-\sin\hat{\varphi}_1^{opt,y}\sin\hat{\theta}_1^{opt,y},-\sin\hat{\varphi}_2^{opt,y}\sin\hat{\theta}_2^{opt,y},\cdots,-\sin\hat{\varphi}_K^{opt,y}\sin\hat{\theta}_K^{opt,y}]$ and $[f_1^{opt,y},\ldots,f_K^{opt,y}]$. Denote the k-th column of $\hat{\mathbf{F}}_x$ and $\hat{\mathbf{F}}_y$ as $\hat{\mathbf{f}}_x(\varphi_k,\theta_k,f_k,f_d)$ and $\hat{\mathbf{f}}_y(\varphi_k,\theta_k,f_k,f_d)$, respectively. We have

$$\begin{aligned}\hat{\mathbf{g}}_{xk}&=-angle(\hat{\mathbf{f}}_x(\varphi_k,\theta_k,f_k,f_d))\\&=[0,2\pi\tau u_k,\ldots,2\pi(P-1)\tau u_k]^T=u_k\mathbf{q}_x,\end{aligned} \tag{35}$$

$$\begin{aligned}\hat{\mathbf{g}}_{yk}&=-angle(\hat{\mathbf{f}}_y(\varphi_k,\theta_k,f_k,f_d))\\&=[0,2\pi\tau v_k,\ldots,2\pi(P-1)\tau v_k]^T=v_k\mathbf{q}_y,\end{aligned} \tag{36}$$

where $u_k=\hat{f}_k^{opt,x}+f_{dk}\cos\hat{\varphi}_k^{opt,x}\sin\hat{\theta}_k^{opt,x}$, $v_k=\hat{f}_k^{opt,y}+f_{dk}\sin\hat{\varphi}_k^{opt,y}\sin\hat{\theta}_k^{opt,y}$, $\mathbf{q}_{xk}=[0,2\pi\tau,\ldots,2\pi(P-1)\tau]^T$, $\mathbf{q}_{yk}=[0,2\pi\tau,\ldots,2\pi(P-1)\tau^T]$. From Eq. (35), we can obtain the estimates of u_k and v_k via the LS method, respectively. The LS fitting amounts to

$$\min_{\mathbf{c}_{xk}}\|\mathbf{E}_{xk}\mathbf{c}_{xk}-\mathbf{g}_{xk}\|_F^2, \tag{37}$$

$$\min_{\mathbf{c}_{yk}}\|\mathbf{E}_{yk}\mathbf{c}_{yk}-\mathbf{g}_{yk}\|_F^2, \tag{38}$$

where $\mathbf{c}_{xk}=[c_{xk0},c_{xk1}]^T$, $\mathbf{c}_{yk}=[c_{yk0},c_{yk1}]^T$, $\mathbf{E}_{xk}=[\mathbf{1}_M,\mathbf{q}_{xk}]$ and $\mathbf{E}_{yk}=[\mathbf{1}_{N-1},\mathbf{q}_{yk}]$. From Eq. (37), we can obtain the estimates of $\mathbf{c}_{xk}$

$$\hat{\mathbf{c}}_{xk}=[\hat{c}_{xk0},\hat{c}_{xk1}]^T=\mathbf{E}_{xk}^{\dagger}\mathbf{g}_{xk}, \tag{39}$$

$$\hat{\mathbf{c}}_{yk}=[\hat{c}_{yk0},\hat{c}_{yk1}]^T=\mathbf{E}_{yk}^{\dagger}\mathbf{g}_{yk}, \tag{40}$$

where $\hat{c}_{xk1}$ and $\hat{c}_{yk1}$ are estimates of u_k and v_k, respectively. The estimates of Doppler from (39) and (40) can be achieved by

$$\hat{f}_{dk}^{opt,x}=(\hat{c}_{xk1}-f_k^{opt,x})/(\cos\varphi_k^{opt,x}\sin\theta_k^{opt,x}),\quad k=1,2,\ldots,K, \tag{41}$$

$$\hat{f}_{dk}^{opt,y}=(\hat{c}_{yk1}-f_k^{opt,y})/(\sin\varphi_k^{opt,y}\sin\theta_k^{opt,y}),\quad k=1,2,\ldots,K. \tag{42}$$

Finally we can get the estimate of Doppler

$$\hat{f}_{dk}=(\hat{f}_{dk}^{opt,x}+\hat{f}_{dk}^{opt,y})/2,\quad K=1,2,\ldots,K. \tag{43}$$

C. THE PROCEDURE OF THE PROPOSED ALGORITHM

The main step of the proposed algorithm can be summarized as follows.

1) The introduction of multi-level delays outputs establishes the fundamental of the dual PARAFAC model (7).

2) Implement the first PARAFAC decomposition on (7) via TALS algorithm and obtain the paired 2-D DOA estimation from $\hat{\mathbf{H}}$.

3) Apply the second PARAFAC decomposition to Eq. (25) and Eq. (26), obtain the estimates of $\hat{\mathbf{A}}_x$ and $\hat{F}_x$, $\hat{\mathbf{A}}_y$ and $\hat{\mathbf{F}}_y$, respectively.

4) Get the Doppler and 2-D DOA matching information via triple matching implementation, e.g. 2-D DOA and frequency, therefore, Doppler is achieved by delay matrices $\hat{\mathbf{F}}_x$ and $\hat{\mathbf{F}}_y$.

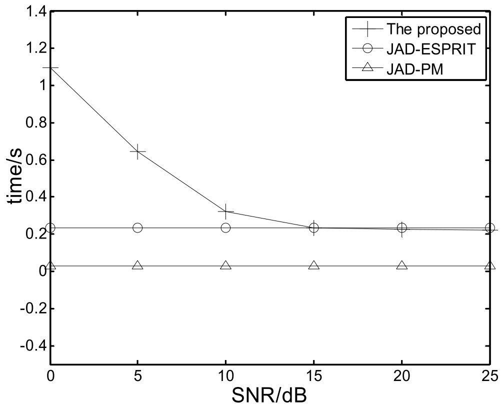

FIGURE 3. Running time comparison under different SNR.

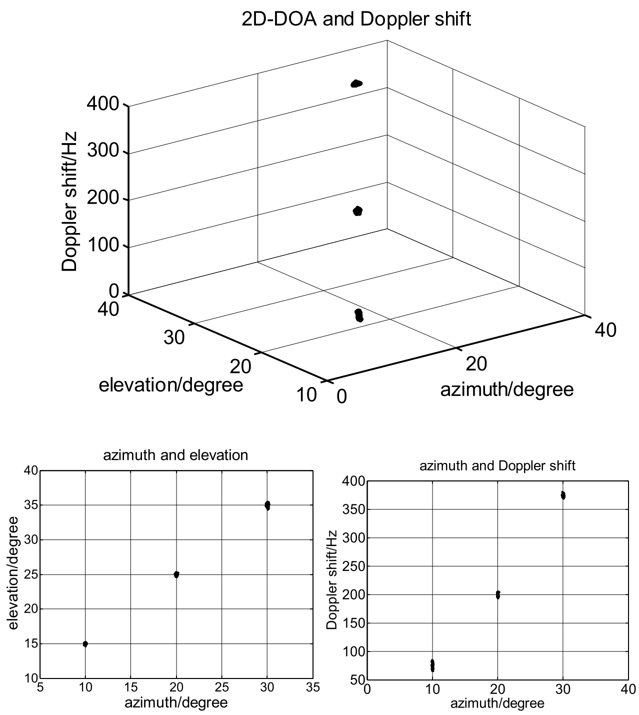

FIGURE 4. 2-D DOA and Doppler estimation for uniform L-shaped array.

IV. COMPLEXITY ANALYSIS

For the proposed algorithm, the complexity for each iteration of the first PARAFAC decomposition is $O[3K^2 + K^2(J + PM+PN+4)+6K^2P((M+N)(4+J)+4J)+12KP(M+N)J]$, while in the second PARAFAC decomposition, each iteration in $\mathbf{G}_x$ and $\mathbf{G}_y$ costs, $O[3K^2+K^2(K+P+M)+6K^2(P(M+K)+MK)+3K^2PM]$, and $O[3K^2+K^2(K+P+N)+6K^2(P(N+K)+NK)+3K^2PN]$, respectively. The complexity of the triple matching implementation and Doppler estimation is $O[2K(K!)+K^2(M+N)]$. So the complexity of the proposed algorithm is $O[n_1(3K^2+K^2(J+PM+PN+4))]$ $+6K^2P((M+N)(4+J)+4J)+12KP(M+N)J+n_{21}(3K^2+K^2(K+P+M)+6K^2(P(M+K)+MK)+3K^2PM)+n_{22}(3K^2+K^2(K+P+N)+6K^2(P(N+K)+NK)+3K^2PN)+2K(K!)+K^2(M+N)$, where n_1 are the iteration times of

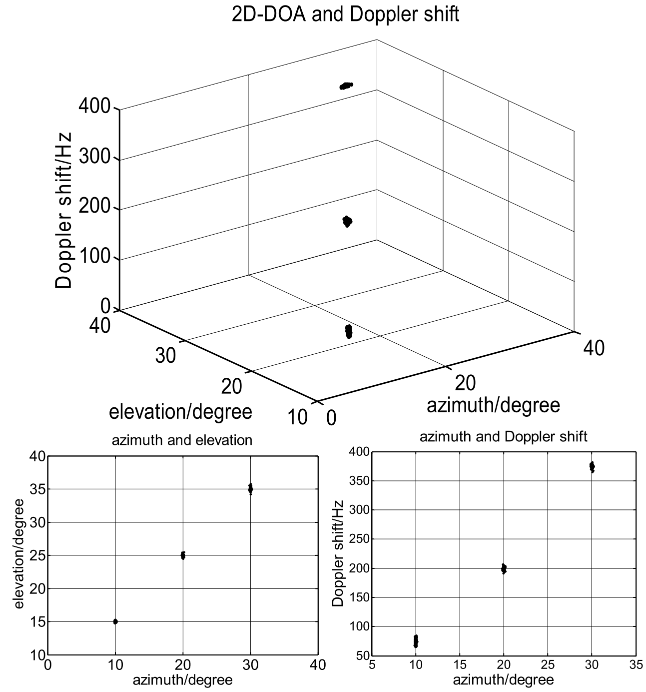

FIGURE 5. 2-D DOA and Doppler estimation for non-uniform L-shaped array.

the first PARAFAC decomposition, n_{21} and n_{22} are the iterations times of the second PARAFAC decomposition. For the sake of clarification, we list the complexity of the proposed algorithm, JAD-ESPRIT algorithm and JAD-PM algorithm in Table 1.

Basically, it is quite difficult to compare the proposed methods with other methods directly since the number of iterations depends on heavily the received data and varies dramatically from a few to even hundreds of iterations, and therefore, it is difficult for one to provide the precise computational complexity. However, the general measure is to numerically compare the CPU runtime of comparable methods as a reference based on the same hardware and software configuration on a computer. In Fig. 3, we present the actual runtime of the comparable algorithms versus SNR, computed by the MATLAB R2015b under the condition of Inter (R) Xeon (R) CPU E5-2620 v3 @2.40GHz and 8GB random access memory, where $M = N = 10, P = 8$. And Fig.3 shows clearly that the proposed algorithm has much close complexity with JAD-ESPRIT as SNR exceeds 15dB because high SNR leads to faster convergence. On the other hand, the JAD-ESPRIT algorithm has the needs for eigenvalue decomposition of the covariance matrix of the received data, which suffers heavy computational load.

V. SIMULATION RESULTS

We consider a scenario of underwater acoustic signal detection and assume that there are three far-field incoherent sources impinge on a L-shaped array, the 2-D

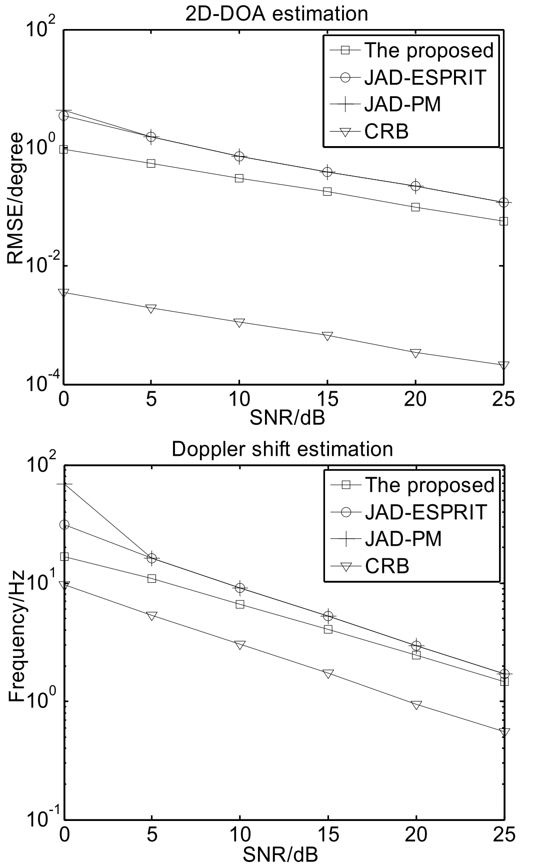

FIGURE 6. **2-D DOA and Doppler estimation performance comparison.**

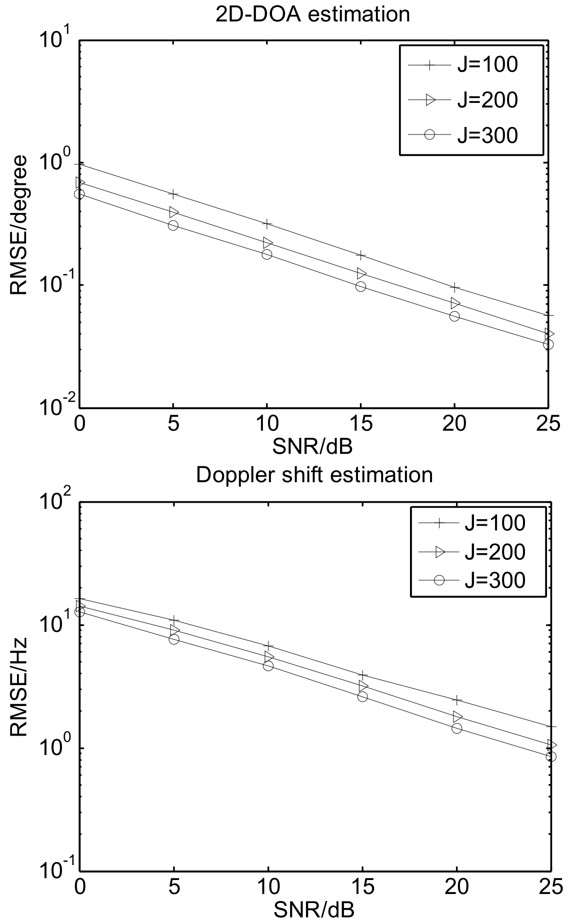

FIGURE 7. **2-D DOA and Doppler estimation performance under different J.**

DOA and frequency of the sources are $(\varphi_1, \theta_1, f_1) = (10°, 15°, 1KHz)$, $(\varphi_2, \theta_2, f_2) = (20°, 25°, 2KHz)$ and $(\varphi_3, \theta_3, f_3) = (30°, 35°, 3\text{KHz})$, respectively. The sources are moving at the speed of $v_1 = 25.5m/s$, $v_1 = 34m/s$ and $v_1 = 42m/s$, respectively. $c = 340m/s$, the Doppler are $f_{d1} = \frac{v_1}{c} f_1 = 75\text{Hz}$, $f_{d2} = \frac{v_2}{c} f_2 = 200\text{Hz}$ and $f_{d3} = \frac{v_3}{c} f_3 = 375\text{Hz}$. J is the snapshots and P is the number of delays. M and N are the numbers of elements of X-subarray and Y-subarray, respectively. In the following examples, the 2-D DOA and Doppler estimation performance of the proposed algorithm is evaluated by the root mean square error (RMSE), which is defined as

$$RMSE_{2-DDOA} = \frac{1}{K}\sum_{k=1}^{K}\sqrt{\frac{1}{L}\sum_{l=1}^{L}[(\hat{\varphi}_{k,l}-\varphi_k)^2+(\hat{\theta}_{k,l}-\theta_k)^2]}, \tag{44}$$

$$RMSE_{Doppler} = \frac{1}{K}\sum_{k=1}^{K}\sqrt{\frac{1}{L}\sum_{l=1}^{L}(\hat{f}_{dk,l}-f_{dk})^2}, \tag{45}$$

where φ_k, θ_k and f_{dk} are the true elevation angle, azimuth angle and Doppler of the k-th source, respectively. $\hat{\varphi}_{k,l}$, $\hat{\theta}_{k,l}$, $\hat{f}_{dk,l}$ are the estimates of φ_k, θ_k and f_{dk} in l-th trial. $L = 1000$is the number of Monte-Carlo trials.

Simulation 1: In this example, we set $M = N = P = 10$, $J = 100$. Fig. 4 and Fig. 5 show the 2-D DOA and Doppler estimation of the proposed algorithm at SNR=15dB. Fig. 4 is the example for uniform L-shaped array and the distance between every adjacent sensor is$d = 0.05m$. While in Fig. 5, the array is non-uniform and the distance between every sensor and the reference element is $d_x = d_y = 0, 0.07, 0.11, 0.14, 0.23, 0.26, 0.264, 0.37, 0.406, 0.45m$. As seen in Fig. 4 and Fig. 5, our algorithm is efficient for both uniform and non-uniform L-shaped array.

Simulation 2: In this example, we compare the parameters estimation performance of the proposed algorithm with JAD-ESPRIT algorithm and JAD-PM algorithm and CRB as well. The array is uniform L-shaped array with $d = 0.05m$, and set $M = N = P = 10$, $J = 100$. From simulation results in Fig.6, we can conclude that the angle and Doppler estimation performance of the proposed algorithm is better than the JAD-ESPRIT and JAD-PM method. It can be observed that the 2-D DOA estimation curve for the proposed method is far higher than the CRB, the reason is that in our paper the 2-D DOA is estimated and paired automatically via the $\mathbf{H}$ matrix only, whose size is $4 \times K$. *Note*: the proposed method

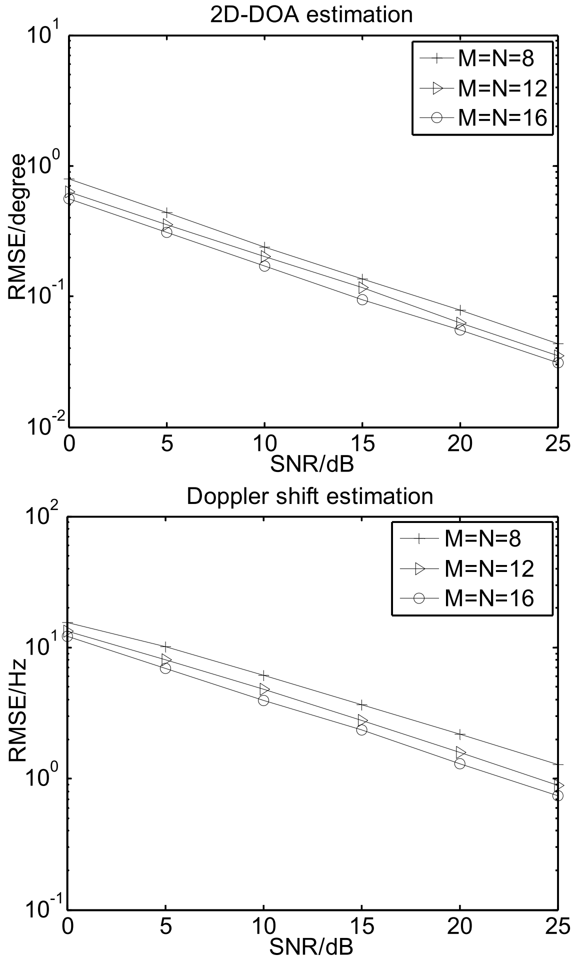

FIGURE 8. 2-D DOA and Doppler estimation performance under different sensor numbers.

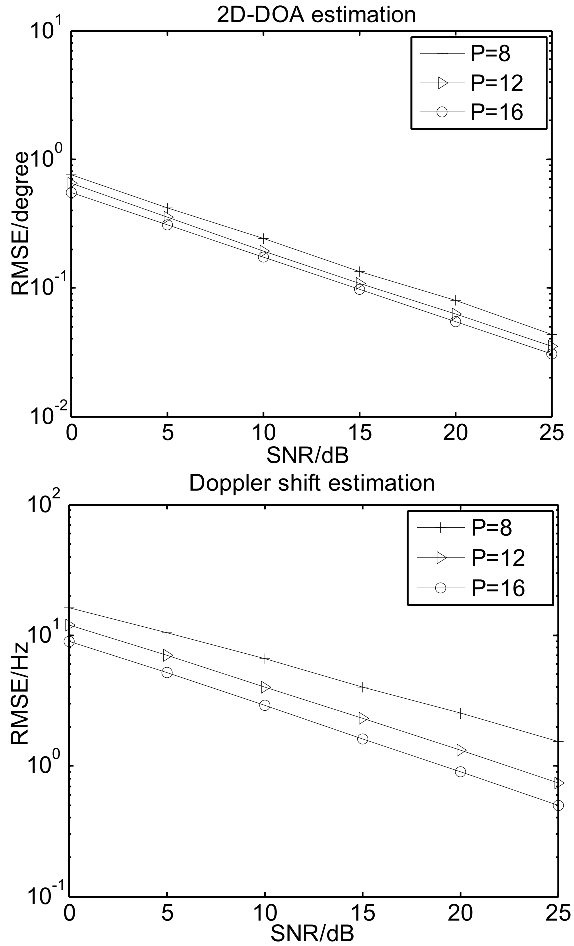

FIGURE 9. 2-D DOA and Doppler estimation performance under different P.

does not use the composite steering matrix $\mathbf{B}$ to estimate 2-D DOA, however, the 2-D DOA CRB is closely related to $\mathbf{B}$. On the other hand, the Doppler estimation curve for the proposed method is relatively closer to the Doppler CRB, the reason is that the Doppler estimation depends on the delay matrices $\mathbf{F}_x$ and $\mathbf{F}_y$ as calculated in (35)-(43).

Simulation 3: Fig.7 shows the 2-D DOA and Doppler estimation performance versus the number of snapshots. In this example, $M = N = P = 10$ with J =100, J =200 and J =300, respectively. It is observed that the estimation performance of both 2-D DOA and Doppler improve with snapshots (J).

*Simulation 4:*Fig.8 shows the 2-D DOA and Doppler estimation performance against the number of array elements. In this example,$P = 10$,$J = 200$ with $M = N = 8$, $M = N = 12$ and $M = N = 16$, respectively. Fig.8 reconfirms that the estimation performance of both 2-D DOA and Doppler gets better with the number of array elements (M, N).

Simulation 5: Fig.9 presents the 2-D DOA and Doppler estimation performance versus P. In this example, $M = N = 10$, $J = 200$ with $P = 8$, $P = 12$ and $P = 16$, respectively. Fig.9 indicates that the estimation performance of both 2-D DOA and Doppler improves as P increases.

VI. CONCLUSIONS

In this paper, we address the problem of joint 2-D DOA and Doppler estimation for L-shaped array, and propose an efficient Dual PARAFAC decomposition method. The proposed method utilizes dual PARAFAC decomposition to estimate parameters matrices, and achieves the 2-D DOA, frequency and Doppler paired with triple matching implementation. The simulation results indicate that the proposed algorithm is effective for both uniform and non-uniform L-shaped array, and the estimation performance outperforms the JAD-ESPRIT algorithm and JAD-PM algorithm. Based on the current research, we would like to test the proposed method using real data in the future work.

APPENDIX A

DEFINATION OF $\mathbf{F_x}$, the equation can be derived, as shown at the top of next page where $f_{dk} = \frac{v_k}{c} f_k$ is the Doppler of the k-th signal.

$$\mathbf{F}_x = \begin{bmatrix} 1 & 1 & \cdots & 1 \\ e^{-j2\pi(f_1+f_{d1}\cos\varphi_1\sin\theta_1)\tau} & e^{-j2\pi(f_2+f_{d2}\cos\varphi_2\sin\theta_2)\tau} & \cdots & e^{-j2\pi(f_K+f_{dK}\cos\varphi_K\sin\theta_K)\tau} \\ \vdots & \vdots & \ddots & \vdots \\ e^{-j2\pi(f_1+f_{d1}\cos\varphi_1\sin\theta_1)_1(P-1)\tau} & e^{-j2\pi(f_2+f_{d2}\cos\varphi_2\sin\theta_2)(P-1)\tau} & \cdots & e^{-j2\pi(f_K+f_{dK}\cos\varphi_K\sin\theta_K)(P-1)\tau} \end{bmatrix}.$$

$$\mathbf{F}_y = \begin{bmatrix} 1 & 1 & \cdots & 1 \\ e^{-j2\pi(f_1+f_{d1}\sin\varphi_1\sin\theta_1)\tau} & e^{-j2\pi(f_2+f_{d2}\sin\varphi_2\sin\theta_2)\tau} & \cdots & e^{-j2\pi(f_K+f_{dK}\sin\varphi_K\sin\theta_K)\tau} \\ \vdots & \vdots & \ddots & \vdots \\ e^{-j2\pi(f_1+f_{d1}\sin\varphi_1\sin\theta_1)_1(P-1)\tau} & e^{-j2\pi(f_2+f_{d2}\sin\varphi_2\sin\theta_2)(P-1)\tau} & \cdots & e^{-j2\pi(f_K+f_{dK}\sin\varphi_K\sin\theta_K)(P-1)\tau} \end{bmatrix}.$$

APPENDIX B

DEFINATION OF $\mathbf{F}_y$, the equation can be derived, as shown at the top of this page where $f_{dk} = \frac{v_k}{c} f_k$ is the Doppler of the k-th signal.

APPENDIX C

Take derivatives of $\boldsymbol{\rho}_{px}$ and $\boldsymbol{\rho}_{py}$ with regards to $\cos\boldsymbol{\theta}_p$, respectively, we have

$$\begin{aligned} &\left.\frac{\partial\boldsymbol{\rho}_{px}}{\partial\cos\boldsymbol{\theta}_p}\right|_{\boldsymbol{\theta}_p=\hat{\boldsymbol{\theta}}_p,\boldsymbol{\varphi}_p=\hat{\varphi}_p} \\ &= \left[\frac{\partial\boldsymbol{\rho}_{px}(1)}{\partial\cos\theta_{p,1}},\ldots,\frac{\partial\boldsymbol{\rho}_{px}(K)}{\partial\cos\theta_{p,K}}\right]\Bigg|_{\boldsymbol{\theta}p} = \hat{\boldsymbol{\theta}}_p, \boldsymbol{\varphi}_p = \hat{\varphi}_p \\ &\quad = [-\cos\hat{\varphi}_{p1}\sin\hat{\theta}_{p1}, -\cos\hat{\varphi}_{p2}\sin\hat{\theta}_{p2},\cdots, \\ &\quad - \cos\hat{\varphi}_{pK}\sin\hat{\theta}_{pK}], \\ &\left.\frac{\partial\boldsymbol{\rho}_{py}}{\partial\cos\boldsymbol{\theta}_p}\right|_{\boldsymbol{\theta}p=\hat{\boldsymbol{\theta}}_p,\boldsymbol{\varphi}_p=\hat{\varphi}_p} \\ &= \left[\frac{\partial\boldsymbol{\rho}_{py}(1)}{\partial\cos\theta_{p,1}},\ldots,\frac{\partial\boldsymbol{\rho}_{py}(K)}{\partial\cos\theta_{p,K}}\right]\Bigg|_{\boldsymbol{\theta}p} = \hat{\boldsymbol{\theta}}_p, \boldsymbol{\varphi}_p = \boldsymbol{\varphi}_p \\ &\quad = [-\sin\hat{\varphi}_{p1}\sin\hat{\theta}_{p1}, -\sin\hat{\varphi}_{p2}\sin\hat{\theta}_{p2},\cdots, \\ &\quad - \sin\hat{\varphi}_{pK}\sin\hat{\theta}_{pK}], \end{aligned}$$

ACKNOWLEDGMENT

The authors would like to appreciate the anonymous reviewers for their highly valuable feedbacks that significantly improve the quality of this paper.

REFERENCES

[1] H. Yu, X. Zhang, X. Chen, and H. Wu, "Computationally efficient DOA tracking algorithm in monostatic MIMO radar with automatic association," *Int. J. Antennas Propag.*, vol. 2014, no. 12, pp. 1–10, 2014.

[2] Y. Fayad, C. Wang, and Q. Cao, "A sequential adaptive method for enhancing DOA tracking performance," *Trans. Nanjing Univ. Aeronaut. Astronaut.*, vol. 33, no. 6, pp. 739–746, 2016.

[3] K. Cui, W. Wu, J. Huang, X. Chen, and N. Yuan, "DOA estimation of LFM signals based on STFT and multiple invariance ESPRIT," *Int. J. Electron. Commun.*, vol. 77, pp. 10–17, Jul. 2017.

[4] L. Xu, R. Wu, X. Zhang, and Z. Shi, "Joint two-dimensional DOA and frequency estimation for L-shaped array via compressed sensing PARAFAC method," *IEEE Access*, vol. 6, pp. 37204–37213, 2018.

[5] R. Shafin, L. Liu, Y. Li, A. Wang, and J. Zhang, "Angle and delay estimation for 3-D massive MIMO/FD-MIMO systems based on parametric channel modeling," *IEEE Trans. Wireless Commun.*, vol. 16, no. 8, pp. 5370–5383, Aug. 2017.

[6] J. D. Lin, W. H. Fang, Y. Y. Wang, and J. T. Chen, "FSF MUSIC for joint DOA and frequency estimation and its performance analysis," *IEEE Trans. Signal Process.*, vol. 54, no. 12, pp. 4529–4542, Dec. 2006.

[7] W. Xudong, "Joint angle and frequency estimation using multiple-delay output based on ESPRIT," *EURASIP J. Adv. Signal Process.*, vol. 2010, no. 1, 2010, Art. no. 358659.

[8] S. Zhongwei X. Zhang, and H. Wu, "Propagator method-based joint angle and frequency estimation using multiple delay output," *ICIC Exp. Lett.*, vol. 2, no. 4, pp. 827–832, 2011.

[9] L. Xu, X. Zhang, and Z. Xu, "Novel blind joint 2D direction of arrival and frequency estimation with L-shaped array," *Int. J. Digit. Content Technol. Its Appl.*, vol. 5, no. 9, pp. 241–250, 2011.

[10] Z. Xiaofei, F. Gaopeng, Y. Jun, and X. Dazhuan, "Angle—Frequency estimation using trilinear decomposition of the oversampled output," *Wireless Pers. Commun.*, vol. 51, no. 2, pp. 365–373, 2009.

[11] J. B. Kruskal, "Three-way arrays: Rank and uniqueness of trilinear decompositions, with application to arithmetic complexity and statistics," *Linear Algebra Appl.*, vol. 18, no. 2, pp. 95–138, 1975.

[12] Y. Wang and G. Leus, "Space-time compressive sampling array," in *Proc. IEEE Sensor Array Multichannel Signal Process. Workshop*, Oct. 2010, pp. 33–36.

[13] M. Yi, P. Wei, and X.-C. Xiao, "Joint estimation of time delays, Doppler shifts and DOAs of multipath signals," in *Proc. Int. Conf. Commun. Circuits Syst.*, Jun. 2004, pp. 822–825.

[14] A. Gunes and M. B. Guldogan, "Joint underwater target detection and tracking with the Bernoulli filter using an acoustic vector sensor," *Digit. Signal Process.*, vol. 48, pp. 246–258, Jan. 2016.

[15] J. Cao, J. Liu, J. Wang, and X. Lai, "Acoustic vector sensor: Reviews and future perspectives," *IET Signal Process.*, vol. 11, no. 1, pp. 1–9, 2016.

[16] X. Zhang, J. Li, H. Chen, and D. Xu, "Trilinear decomposition-based two-dimensional DOA estimation algorithm for arbitrarily spaced acoustic vector-sensor array subjected to unknown locations," *Wireless Pers. Commun.*, vol. 67, no. 4, pp. 859–877, 2012.

[17] W. Xudong, X. Zhang, J. Li, and J. Bai, "Improved ESPRIT method for joint direction-of-arrival and frequency estimation using multiple-delay output," *Int. J. Antennas Propag.*, vol. 2012, no. 1, 2012, Art. no. 309269.

[18] N. D. Sidiropoulos, L. De Lathauwer, X. Fu, K. Huang, E. E. Papalexakis, and C. Faloutsos, "Tensor decomposition for signal processing and machine learning," *IEEE Trans. Signal Process.*, vol. 65, no. 13, pp. 3551–3582, Jul. 2017.

[19] J. Lin, X. Ma, S. Yan, and C. Hao, "Time-frequency multi-invariance ESPRIT for DOA estimation," *IEEE Antennas Wireless Propag. Lett.*, vol. 15, pp. 770–773, Aug. 2016.

[20] S. Ren, X. Ma, S. Yan, and C. Hao, "2-D unitary ESPRIT-like direction-of-arrival (DOA) estimation for coherent signals with a uniform rectangular array," *Sensors*, vol. 13, no. 4, pp. 4272–4288, 2013.

RIHENG WU (M'12) received the Ph.D. degree in measurement technology and instruments from the Beijing Institute of Technology, Beijing, China, in 2007.

He was a Research Associate Fellow with the Department of Electrical Engineering and Computer Science, The University of Tennessee, Knoxville, TN, USA, from 2007 to 2008. From 2009 to 2015, he was with hi-tech companies in MO, KS, USA, including Leggett and Garmin International Inc., where he owned two authorized U.S. patents. Since 2016, he has been with the Information Engineering Department, Wenjing College, Yantai University, Yantai, China, where he is currently a Full Professor. His research interests include signal processing in communication and radar, array signal processing, optimizations. Dr. Wu serves as a member of the Technical Program Committees of numerous IEEE conferences, including ICC (2011 and 2012), WCNC (2009, 2010, 2011, 2012, 2013, and 2017), CCNC (2011, 2012, and 2018), APMC2017, and VTC. He serves as an Editor of the *International Journal of Computing and Digital Systems*-V7 (IJCDS'018), *Journal of Engineering and Computer Innovations* (JECI), *The Magazine of the IEEE Vehicular Technology Society*, in 2010.

LE XU received the B.Eng. degree from the Nanjing University of Aeronautics and Astronautics, Nanjing, China, in 2016, where he is currently pursuing the master's degree in communication and information systems with the College of Electronic and Information Engineering. His current research interests include array signal processing and compressed sensing theory.

ZHENHAI ZHANG received the B.Eng. degree from the Harbin University of Science and Technology (HUST), Harbin, China, in 1997, and the M.S. and Ph.D. degrees from the School of Mechatronics Engineering, Beijing Institute of Technology (BIT), Beijing, China, in 2004 and 2008, respectively.

From 2010 to 2011, he was a Postdoctoral Researcher with Fukuda Laboratory, Department of Micro-Nano Systems Engineering, Nagoya University, Japan. In 2012, he joined the School of Mechatronics Engineering, Beijing Institute of Technology, where he is currently an Associate Professor. He has authored or coauthored more than 55 peer-reviewed journal publications and conference papers. He held over 25 invention patents. His research areas include MEMS/NEMS sensors and test technology, panorama sensor, bionic robot, locomotive robot, tip-based precision micro/nano-manipulation systems, bio-inspired robotics, micro/nano-robotics, and micro/nano systems for biomedical applications.

Dr. Zhang has served as a Council Member of Sensor Branch of the China Instrument and Control Society, a Committee Member of the Optoelectronic Technology Professional Committee of Chinese Society of Astronautics, an Editorial Board Member of Computer Measurement and Control, and a Project Evaluation Expert of the National Natural Science Fund Committee.

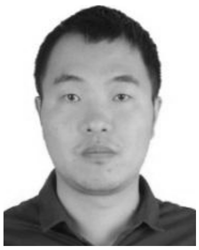

YANGYANG DONG was born in Bengbu, Anhui, China. He received the B.Eng. and Ph.D. degrees in electronic science and technology from Xidian University, Xi'an, China, in 2012 and 2017, respectively. Since 2017, he has been a Lecturer with the School of Electronic Engineering, Xidian University, where he also held a postdoctoral position. His current research interests include array signal processing, multilinear algebra, and information geometry.